Fossil Record 14 (2) 2011, 153–169 / DOI 10.1002/mmng.201100005

WILEY-VCH

museum für naturkunde

Nutrient dynamics and oceanographic features in the central Namibian upwelling region as reflected in δ^{15}N-signals of suspended matter and surface sediments

Sandra Meisel[1], Ulrich Struck*[, 1] and Kay-Christian Emeis[2]

[1] Museum für Naturkunde, Leibniz-Institut für Evolutions- und Biodiversitätsforschung an der Humboldt-Universität zu Berlin, 10115 Berlin, Germany, e-mail: Ulrich.Struck@mfn-berlin.de
[2] Institut für Biogeochemie und Meereschemie, Universität Hamburg, Bundesstr. 55, 20146 Hamburg, Germany

Received 15 November 2010
Accepted 22 February 2011
Published 3 August 2011

Abstract

The study deals with the modern situation of the northern Benguela Upwelling, directing particular attention to the shelf region off central Namibia (21 to 24° S). At the centre of the investigation is the comparison of δ^{15}N-records in surface sediments ($\delta^{15}N_{sediment}$) with suspended particulate matter ($\delta^{15}N_{SPM}$) from the surface ocean. In addition to that, water column profiles (including hydrographic data) provide an insight into changes of $\delta^{15}N_{SPM}$ with depth and elucidate potential offsets between $\delta^{15}N_{SPM}$ and $\delta^{15}N_{sediment}$. The parallel spatial trend of $\delta^{15}N_{sediment}$ and surface ocean $\delta^{15}N_{SPM}$ shows that secondary processes are not so pronounced as to obliterate the signal generated in the surface waters. Highest δ^{15}N-signatures are found right off the coast where water temperatures are lowest. Concomitantly high productivity rates and low bottom oxygen suggest the upwelling of denitrified source waters. With increasing distance offshore, δ^{15}N declines unexpectedly, reaching a minimum above the shelf break. Beyond that, the trend reverses to "normal" with δ^{15}N-signals continuously increasing towards the mesopelagic ocean. The decrease in $\delta^{15}N_{sediment}$ and surface ocean $\delta^{15}N_{SPM}$ with increasing distance to the coast disagrees with the concept of Rayleigh fractionation kinetics, viz. the progressive ^{15}N-enrichment of the nitrate pool as it is gradually used up by phytoplankton growth. On the basis of the available evidence, the downward trend of δ^{15}N results from decreased relative nitrate consumption, resting on a combination of reduced primary production and the existence of an ulterior source of nutrients. Nutrient replenishment seems to occur via an additional upwelling front at the edge of the shelf as well as tapping of subsurface nitrate through sufficiently deep penetration of wind- and wave-induced mixing over large areas of the shelf. Both mechanisms are considered capable of working against the expected nutrient drawdown (i.e. ^{15}N-enrichment) as surface waters travel offshore. It is important to keep these caveats in mind when interpreting δ^{15}N-variations in sediment cores retrieved from this area.

Key Words

Benguela Current
denitrification
nitrogen isotopes
nutrient utilisation
two-celled upwelling
SST

Introduction

The role of eastern boundary upwelling areas in the global climate system far outweighs their modest regional extent. The upwelling of cold and nutrient-rich subthermocline waters supports a powerful biological pump and the sequestration of organic carbon on a large scale (e.g. Berger et al. 1989; Berger & Wefer 2002). Much effort has already been put into a deeper understanding of the Benguela upwelling system as a whole (e.g. Chapman & Shannon 1985; Shannon & Nelson 1996; Shannon & O'Toole 1998). Our investigation focuses on the central Namibian coastal section with particular emphasis on the shelf region, which has been largely neglected in literature so far.

---

* Corresponding author

Information about productivity patterns is derived from C_{org}/N ratios and N-contents in suspended matter as well as from the amount of total organic carbon (TOC) in the surface sediments. Temperature records (recorded in the sediments as well as through direct measurements) reflect the intensity and spatial extent of upwelling.

The main insight into nutrient dynamics and oceanographic features comes from the nitrogen isotope ratios of surface sediments ($\delta^{15}N_{sediment}$) and suspended particulate matter (SPM) from the overlying water column ($\delta^{15}N_{SPM}$). As for the Namibian shelf, this is actually the first time that such a compilation of surface sediment and water column data is presented. The influence of early alteration processes is investigated by tracking downward variations of $\delta^{15}N_{SPM}$ from the sea surface to the seafloor.

Over the last years, δ^{15}N-records have gained growing importance in the study of marine nutrient regimes and food webs. However, the value of $\delta^{15}N_{sediment}$ as a potent biomarker in palaeo-studies depends on the sound knowledge about fractionation-relevant processes involved. Investigating spatial and vertical changes in δ^{15}N, combining data from sediments and suspended matter, may hold some valuable clues to the principle controls on δ^{15}N above the central Namibian shelf. This helps to evaluate the usefulness of $\delta^{15}N_{sediment}$ in ancient sediments and gets particularly useful when it comes to interpreting biological and physical processes operating in the ocean at times that we lack direct insight in the water column (e.g. Meisel et al. 2011).

Nitrogen dynamics and nitrogen isotopes as a proxy parameter

Nitrate (NO_3^-) dominates the oceanic pool of combined nitrogen and supports most of the primary production (Montoya 1994). As long as nutrients are in abundant supply, nitrogen isotopes are fractionated when assimilated by phytoplankton (Ostrom et al. 1997). Phytoplankton typically results depleted in ^{15}N (by ± 5 ‰) relative to the inorganic source nitrogen used for growth. According to Rayleigh fractionation kinetics the remaining NO_3^--pool becomes progressively enriched in ^{15}N and with it the primary producers taking up nutrients from that pool (e.g. Wada & Hattori 1978; Wada 1980; Montoya 1994; Waser et al. 1998). The greater the distance to the nutrient source, by inference, the higher δ^{15}N in both nitrate and the primary product. Without other processes interfering (such as nitrogen fixation, denitrification, etc.), high δ^{15}N-values are thus associated with low nitrate concentrations and vice versa. Owing to this relationship, δ^{15}N-records were extensively used as a proxy of relative nitrate utilisation in the photic zone, sometimes holding valuable clues about ocean circulation and trade wind pattern (e.g. Francois et al. 1992; Altabet & Francois 1994; Montoya 1994; Montoya & McCarthy 1995; Voss et al. 1996; Holmes et al. 1998, 1999, 2002; Pichevin et al. 2005).

Study area

Coastal upwelling

The Benguela Current is the eastern boundary current of the South Atlantic anticyclonic gyre. Its eastern periphery is characterised by an upwelling area with a pronounced negative surface temperature anomaly found between 15 and 34° S (Shannon 1985; Shannon & Nelson 1996). Figure 1 provides an insight in the modern large-scale flow pattern.

Upwelling concentrates on a number of cells along the southwest African coast. The principal centre is in the vicinity of Lüderitz (27° S) where strong upwelling occurs throughout the year. The zone represents an environmental boundary between the northern and southern Benguela, which represent two quasi-independent subsystems (Shannon & Nelson 1996; Shannon & O'Toole 2003; Mohrholz et al. 2008). The area under investigation lies within the Central Namibian Upwelling Cell in the northern Benguela (Shannon & Nelson 1996).

The northern Benguela exhibits a late winter-spring maximum (September to November) and summer minimum (January to March) in upwelling activity (Hart & Currie 1960; Stander 1964; Nelson & Hutchings 1983; Shannon 1985). Upwelling is induced by the trade winds (e.g. Lutjeharms & Meeuwis 1987). Surface waters are dragged offshore, giving rise to a pressure deficit that is compensated for by the advection of deeper water masses travelling up the shelf. Seasonal variability nonetheless, this cross-shelf circulation is maintained all year round. The offshore-directed surface layer is thickest in austral winter when upwelling is strongest (up to 35 m; in austral summer reaching 20 m only). At the same time the onshore compensation flow covers the entire water column below the surface mixed layer. In summer the onshore flow slackens and vanishes completely near the bottom (Mohrholz et al. 2008).

Upwelling taps water from up to 200 m depths (Calvert & Price 1971; Mohrholz et al. 2008). The upwelled water represents a mélange of two upper central water masses, namely nutrient-rich and oxygen-poor South Atlantic Central Water (SACW) and well-oxygenated and nutrient-poor Eastern South Atlantic Central Water (ESACW) (Table 1) (Mohrholz et al. 2008). SACW originates from the Brazil-Malvinas Confluence region of the Subtropical Convergence in the Southwest Atlantic. It is transported within the subtropical gyre and the equatorial current system into the Angola Dome region where continuous remineralisation of organic matter (OM) reduces its O_2-content while enriching its nutrient loads. From there, it is eventually advected along the shelf into the northern Benguela via the Angola Current, or, more precisely, via its southward continuation in the form of a poleward undercurrent penetrating through the Angola-Benguela Front (ABF). As regards the maximum southward reach of the undercurrent, 27° S is considered a good estimate (Mohrholz et al. 2008). Owing to its low oxygen content, SACW is held partly responsible

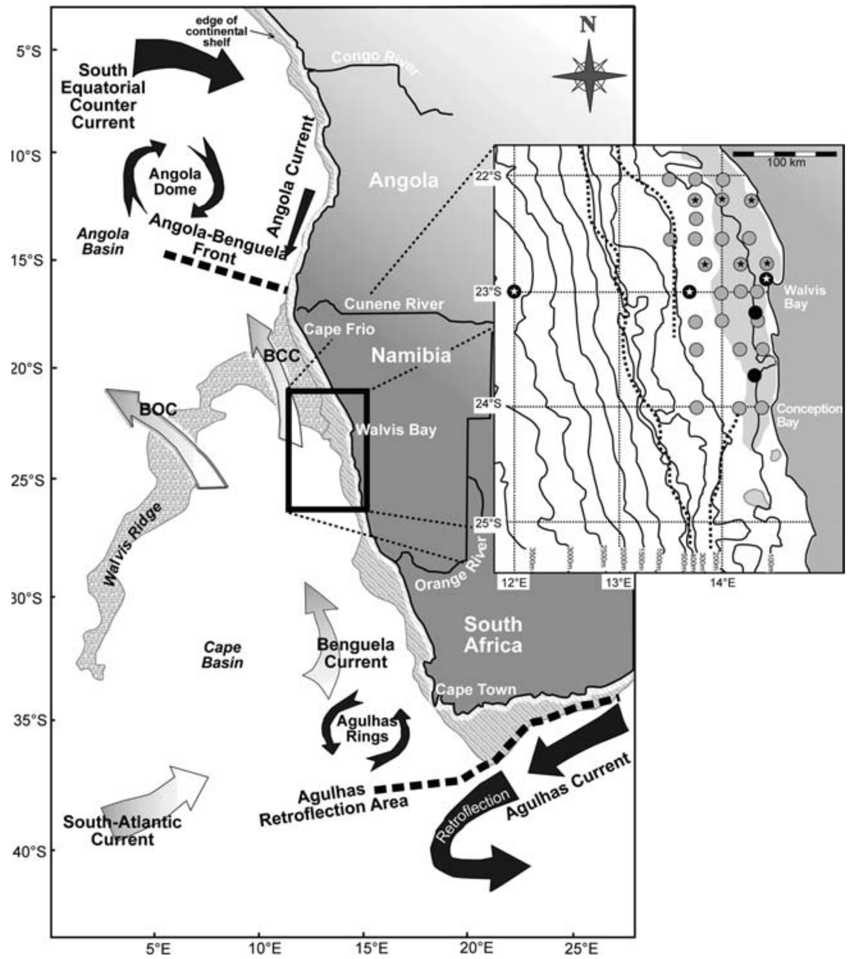

Figure 1. The Benguela Upwelling is bordered by highly dynamic warm water regimes at both of its ends, i.e. the Angola-Benguela Front (ABF) in the north and the Agulhas Retroflection area in the south. The warm South Equatorial Counter Current (SECC) flows south-eastward towards the Angola Basin at subsurface depths. It reaches the surface at around 10° S where it continues southward as the Angola Current (Moroshkin et al. 1970). The Benguela Current splits into the Benguela Oceanic Current (BOC) and the Benguela Coastal Current (BCC) at approximately 28° S. The BOC is separated from the SECC by the Angola Dome, a large cyclonic gyre, which is considered the remote source of hypoxic, nutrient-rich SACW (Mohrholz et al. 2008). The BCC travels parallel to the coast and turns west at the ABF (Stramma & Peterson 1989). The ABF migrates seasonally between about 14 and 17° S and separates the oligotrophic tropical ecosystem in the north from the nutrient-rich Benguela upwelling system in the south (Summerhayes et al. 1995). Still, it is no strong barrier and allows the injection of SACW into the northern Benguala via a poleward undercurrent (Mohrholz et al. 2008). Light arrows denote cold surface currents, the darker arrows denote warm surface currents (map modified after Holmes et al. 1999). The small chart zooms in on the area under investigation and shows where water column profiles for the collection of SPM and hydrographic data were taken (black dots M57-3 expedition; grey dots AHAB 05 cruise). Figure 3 provides details about the locations highlighted. The diatomaceous muds, coating the inner shelf up to approximately 150 m depth, are shaded grey. The dotted lines denote the double shelf break, which characterises much of the central Namibian region (after Bremner & Willis 1993).

Table 1. The water mass properties of South Atlantic Central Water (SACW) and Eastern South Atlantic Central Water (ESACW), defining both end-members of the source water in the northern Benguela.

	SACW	ESACW
	Mohrholz et al. (2008)	Poole & Tomczak (1999)
temperature (°C)	8.0–16.0	6.0–14.4
oxygen (μmol/l)	22.4–68.4	249.3–300.1
nitrate (μmol/l)	21.9–37.9	0–11.8

for the sub- to anoxic condition above the shelf (Chapman & Shannon 1987; Shannon & Nelson 1996).

The second water mass, ESACW, is formed in the Agulhas Retroflection area in the south. It represents a mixture of central waters from the subtropical gyre and varying amounts of warm Indian Ocean Central (Agulhas) Water injected into the South Atlantic through the Agulhas Current (Gordon 1986; Shannon & O'Toole 2003; Mohrholz et al. 2008). ESACW is carried northward along the upper continental slope and edge of the shelf by the Benguela current itself (Gordon 1986; Mohrholz et al. 2008).

The northward flowing ESACW and southward flowing SACW meet in the large transition area between the ABF and the Lüderitz Upwelling, being mixed by cross-shelf circulation (see above). As with cross-shelf circulation, Mohrholz et al. (2008) reported a clear seasonal variability in the intensity of the longshore current components and the proportions of ESACW and SACW off Walvis Bay. In austral winter, northward advected ESACW shifts the frontal zone between both water masses equatorward and most of the SACW is removed. During summer, when upwelling slackens and the ABF moves southward and weakens, the percentage of hypoxic SACW on the northern Benguela shelf rises.

Shelf anoxia

The adverse influence of SACW on the local oxygen status is evidenced by the strong inverse correlation between SACW fraction and oxygen concentration over the entire northern Benguela shelf (Mohrholz et al. 2008). Still, SACW is not the sole reason for the lack of oxygen. The extent of the oxygen deficiency also depends on local oxygen consumption associated with remineralisation of sinking organic detritus. High primary production induces great oxygen demand down in the water column and often brings about severe anoxia over large areas of the southwest African shelf (Chapman & Shannon 1985; Codispoti & Christensen 1985; Shannon & O'Toole 1998; Tyrrell & Lucas 2002; Gaye-Haake et al. 2005). The subsurface transport of oxygen-rich ESACW from the shelf edge onto the shelf theoretically balances the oxygen consumption below the surface mixed layer. During summer, when upwelling-favourable winds weaken, however, the Ekman compensation flow is restricted to intermediate depths with the bottom layer being excluded. Weaker advection of oxygenated ESACW in combination with pronounced intrusions of hypoxic SACW (see introduction) and continuing oxygen demand due to respiration makes the summer ventilation less effective than in winter (Mohrholz et al. 2008). In fact, the occurrence of widespread shelf anoxia is a seasonally recurrent feature.

Material and methods

The investigation is based on an extensive compilation of (i) hydrographic measurements, (ii) suspended particulate matter and (iii) surface sediments. (i) and (ii) include data from the sea surface and the water column. See Table 2 for a clear listing of the respective parameters analysed.

Water sampling (hydrographic data and suspended particulate matter)

Samples and measurements were taken during METEOR cruise M57–3 (15/03/2003 to 08/04/2003) and the AHAB 05-expedition (RV Alexander von Humboldt; Angola-Benguela; 17/03/2004 to 05/04/2004) in late austral summer. At that time of the year, upwelling typically slackens (see introduction). Most of the data derive from the shelf between 22 and 25° S and only few reach up to 250 km offshore (Table 2).

The investigation is based on suspended particulate matter (SPM) collected along with hydrographic data (temperature, oxygen, chlorophyll) at 31 water column profiles (Fig. 1). Double in amount are SPM-samples from the surface waters (Fig. 4A) and measurements of the sea surface temperature (SST) (Fig. 2A).

Water sampling and hydrographic measurements were done by means of a CTD (conductivity-temperature-depth)-Rosette-water-sampling-system equipped with an oxygen sensor (Sea-Bird Electronics, Bellevue, WA) and a Haardt Chlorophyll detector (Lavik et al. 2004). The sensor was calibrated by manual Winkler titration. CTD-measurements were taken at roughly 1 m-intervals.

Water samples were taken at various depths with SPM being obtained by filtration of 0.2 to 2 litres of seawater through pre-combusted glass fibre filters (Whatman GFF 0.8 μm) (NB: The term 'suspended particulate matter' includes both sinking and suspended matter). Carbonate-carbon was removed in a vapour of concentrated hydrochloric acid. Prior to measurement the filters were wrapped in tin-foil vessels. The isotopic composition of nitrogen (δ^{15}N) and the total weight percent (wt%) of organic carbon (C_{org}) and nitrogen were determined in a Thermo NC2500 Elemental Analyser connected to an isotope-ratio mass-spectrometer (Finnigan, Delta Plus). The reference gas was pure N_2 calibrated against IAEA-standards N-1 and N-2. In

Table 2. Compilation of the sample material and proxies. The number of measurements, or rather, samples is also shown (= *n*). Origin of the data: a) Most of the data derive from the shelf between 22 and 25° S. Only few reach up to 250 km offshore. b) The profiles derive nearly exclusively from the inner shelf area between 22 und 24° S. c) The sediments span a broader coastal section than the surface ocean SPM-data, reaching from latitude 19 to 30° S. At the same time they reach far beyond the edge of the shelf (TOC up to 230 km, SST and $\delta^{15}N_{sediment}$ up to ± 1000 km offshore). Source studies of previously published data are mentioned.

hydrographic measurements		SPM		surface sediments c)	
surface water a) (*n* = 63)	water column profile b) (*n* = 28)	surface water a) (*n* = 62)	water column profile b) (*n* = 31)		
temperature	temperature (°C)	$\delta^{15}N_{SPM}$ (‰)	$\delta^{15}N_{SPM}$ (‰)	$\delta^{15}N_{sediment}$ (‰) Emeis et al. (2009) Pichevin et al. (2005)	(*n* = 98)
	oxygen (ml/l)	PN (mg/l)	PN (mg/l)	SST (UK-37) (°C) Emeis et al. (2009)	(*n* = 123)
	chlorophyll *a* (mg/l)	POC (mg/l) C_{org}/N (molar)	C_{org}/N (molar)	TOC (%) Mollenhauer et al. (2002)	(*n* = 68; 43 yet unpubl.)

replication measurements, the standard deviation of the lab standard (peptone) did not exceed ±0.2 ‰. Nitrogen isotope ratios are reported in the conventional δ-notation in per mil (‰) with respect to the atmospheric N_2-standard (AIR) (Mariotti 1983).

Surface sediment samples

The term 'surface sediment' denotes the upper 1 cm of sediment. In the diatomaceous muds (see below), where sedimentation rates average 1 mm/a (Bremner & Willis 1993), 1 cm of sediment corresponds to the last 10 years.

The sediment samples span a broader coastal section (latitude 19 to 30° S) than the surface ocean SPM-data and reach far beyond the edge of the shelf. Most sediment data has already been published by various authors (see Table 2). The compilation in one single set of data provides the hitherto most comprehensive spatial image of the central Namibian shelf and slope. Besides, from the comparison with $\delta^{15}N_{SPM}$ we expect novel insights into the transfer of pelagic $\delta^{15}N$-signals to the sea floor.

$\delta^{15}N_{sediment}$ analyses were made on untreated sedimentary material (Pichevin et al. 2005; Emeis et al. 2009 and references therein). SSTs were reconstructed by means of the alkenone palaeo-temperature index UK'37 (Emeis et al. 2009 and references therein). TOC (wt%) from Mollenhauer et al. (2002) is complemented by hitherto unpublished data from METEOR cruise M48–2 (05/08/2000 to 23/08/2000) and RV POSEIDON cruise 250 (06/04/1999 to 28/04/1999).

As a result of the high primary production rates, the shelf sediments are predominantly of biogenic nature. The majority of the samples derive from the organic-rich diatomaceous muds (average opal 54 wt%; average OM 10 wt%; Bremner & Willis 1993) running parallel to the coast (Fig. 1). The mud belt coats the inner shelf up to 150 m depth and thickens to more than 10 m in coastal vicinity (Struck et al. 2002; Brüchert et al. 2004; Emeis et al. 2004). The outer shelf and upper slope are covered by a calcareous facies (> 50 wt % $CaCO_3$) (Bremner & Willis 1993). Towards the shelf break, strong bottom currents impede the deposition of sediments and the sea bottom often consists of hard ground (Brüchert et al. 2004).

Results

Hydrographic data

The SST contour plot is based on 63 CTD-measurements (Fig. 2A). The sampling depths rarely exceed 5 m. SSTs range from roughly 12.5 to 19 °C, with increasing temperatures towards the open ocean. The fact that the gradient along latitude 23° S is that weak is consistent with slackened upwelling at that time of the year. Towards the Lüderitz Cell (27° S) in the south, where upwelling occurs throughout the year, the SST-gradient is much more pronounced indicating upwelling of cold subsurface waters (± 12.5 °C) in the immediate vicinity of the coast.

Figure 3 displays a selection of 9 water column profiles analysed in this study. Their locations are marked with a star in Figure 1. The profiles lie on three east-west-oriented transects and provide an insight in the water column properties at various distances to the coast. If existing, the thermocline is situated between 10 and 30 m depth (Figs 3B–C). In the shallow coastal waters, however, stratification is usually rather weak and offsets between surface and bottom water temperatures rarely exceed 2 °C (Figs 3D–G). Further offshore, the temperature offsets and the thermocline are generally more pronounced. Oxygen declines more or less abruptly below the thermocline and comes close to zero above the ground (Fig. 3).

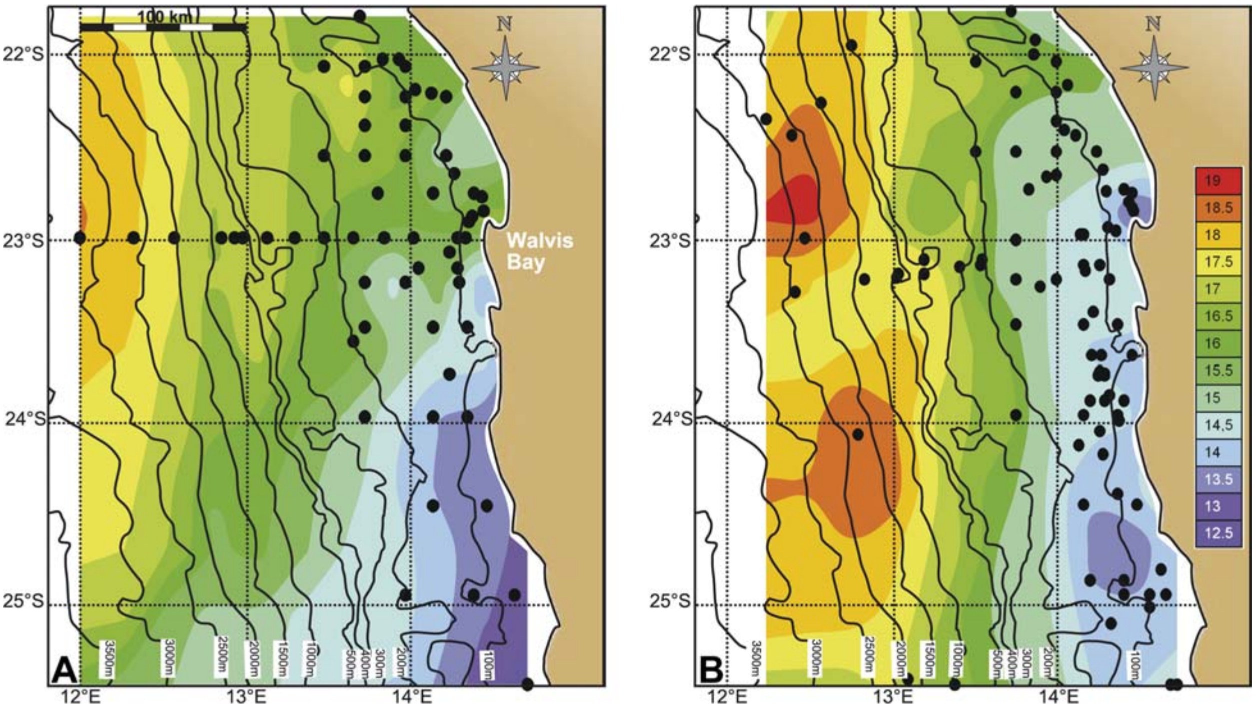

Figure 2. Spatial distribution of SST (°C) reconstructed by means of CTD-measurements (**A**) and sedimentary alkenone (UK'37) data (**B**). The UK'37-record mirrors two centres of upwelling: the seasonally active Central Namibian Cell, located between 22.7 and 24.5° S, and the Lüderitz Cell further south (Shannon & Nelson 1996). The CTD-data bear only witness to the latter.

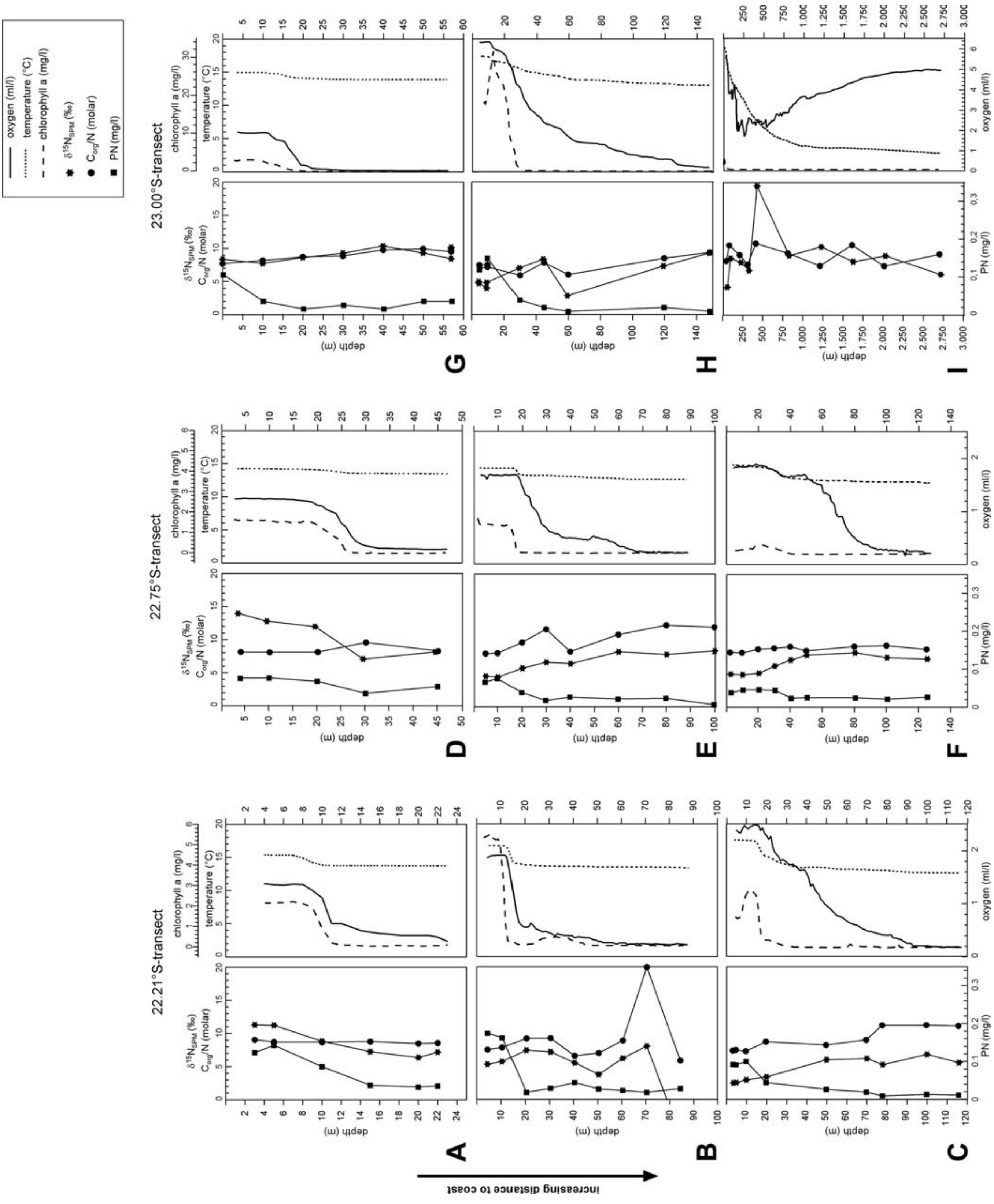

Figure 3. The locations of the profiles and corresponding transects (22.21° S; 22.75°S; 23.00° S) are highlighted in Figure 1. With each transect, the distance to the coast increases from top to bottom. Characteristics of filtration-derived SPM ($\delta^{15}N_{SPM}$, [PN], C_{org}/N) in the left chart are shown along with the CTD-derived hydrographic measurements (temperature, oxygen and chlorophyll content) in the right chart. Profiles A–F were taken during the AHAB 05-cruise, profiles G–I during the M57-3 expedition. Oxygen and chlorophyll were many times higher during Meteor cruise M57-3 than during AHAB 05 (note the larger scale for oxygen and chlorophyll in the 23° S-transect). Such variability is not unusual and testifies to the highly dynamic nature of the region. **A.** 14.25° E/22.21° S; water depth (w.d.) 27 m; **B.** 14.00° E/22.21° S; w.d. 89 m; **C.** 13.75° E/22.21° S; w.d. 120 m; **D.** 14.42° E/22.75° S; w.d. 51 m; **E.** 14.17° E/22.75° S; w.d. 108 m; **F.** 13.83° E/22.75° S; w.d. 134 m; **G.** 14.39° E/22.91° S; w.d. 59 m; **H.** 13.68° E/22.99° S; w.d. 151 m; **I.** 12.00° E/23.00° S w.d. not mentioned.

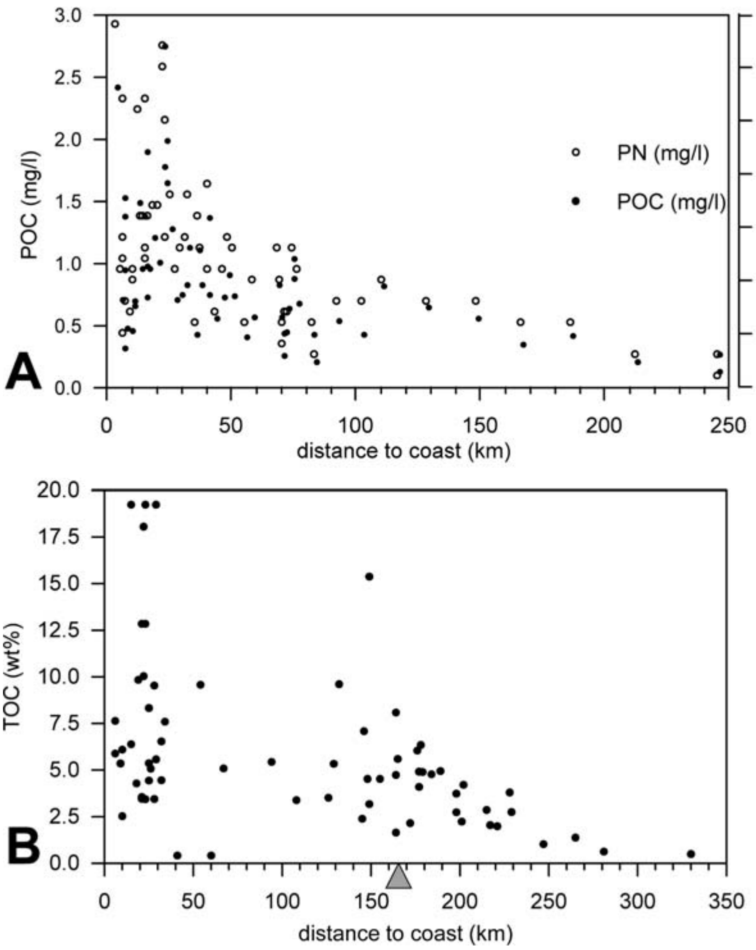

Figure 4. A. [POC] and [PN] in the surface water layer (between latitude 22 and 25.5° S) vs. distance to coast; **B.** [TOC] in the surface sediments (between latitude 19 and 28° S) vs. distance to coast. Above the lower shelf break (see triangle), [TOC] exhibits a minor peak. Note that the sediment data reach slightly further offshore than the data in (A).

Suspended particulate matter (SPM)

Concentrations. Due to the absence of terrestrial material (see below) variations in the amount of particulate nitrogen (PN) and particulate organic carbon (POC) are regarded as an indication of varying primary production rates.

[POC] (particulate organic carbon) in the surface waters ranges from 0.1 to 2.8 mg/l and [PN] (particulate nitrogen) from 0.01 to 0.34 mg/l (Fig. 4A). The oceanward decline in [PN] and [POC] in the upper water layers is clearly visible in Figures 4A and 5.

Both chlorophyll (chl *a*) and [PN] decrease with depth. The CTD-measurements show that the decline in chlorophyll tends to be bound to the thermocline (Figs 3A–E). Around longitude 13.75° E, however, there is a deep chlorophyll maximum (DCM) at the depth of the thermocline (Figs 3C, F, H). DCM are a common feature in many regions of the tropical Atlantic (Ravelo & Fairbanks 1992). The phenomenon was observed during both METEOR cruise M57–3 and the AHAB 05-expedition and vanishes south of 23° S.

$\delta^{15}N_{SPM}$. Surface water $\delta^{15}N_{SPM}$ ranges from roughly 1 to 16 ‰ and decreases with increasing distance to the coast (Figs 6A, 7) (NB: The $\delta^{15}N_{SPM}$-range is more or less comparable to values from the Peru Upwelling

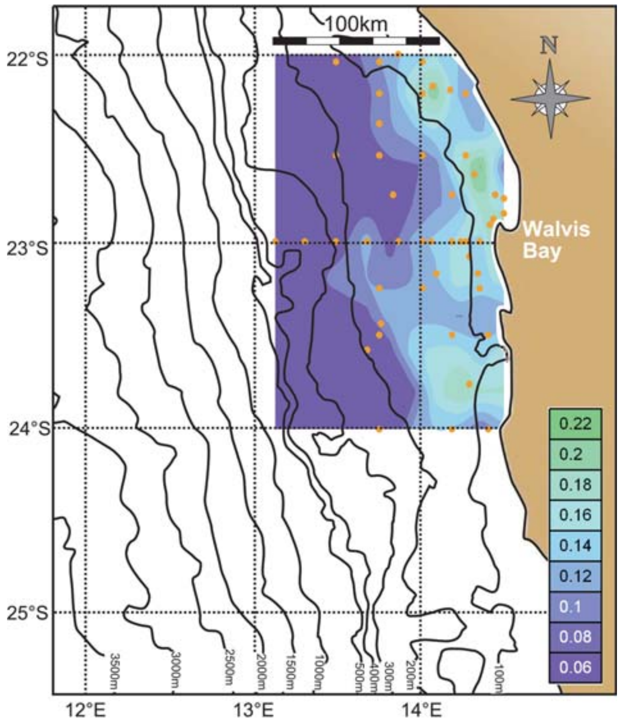

Figure 5. Spatial distribution of [PN] in surface water layer in mg/l. Concentrations are highest in vicinity to the coast and decrease towards the open ocean.

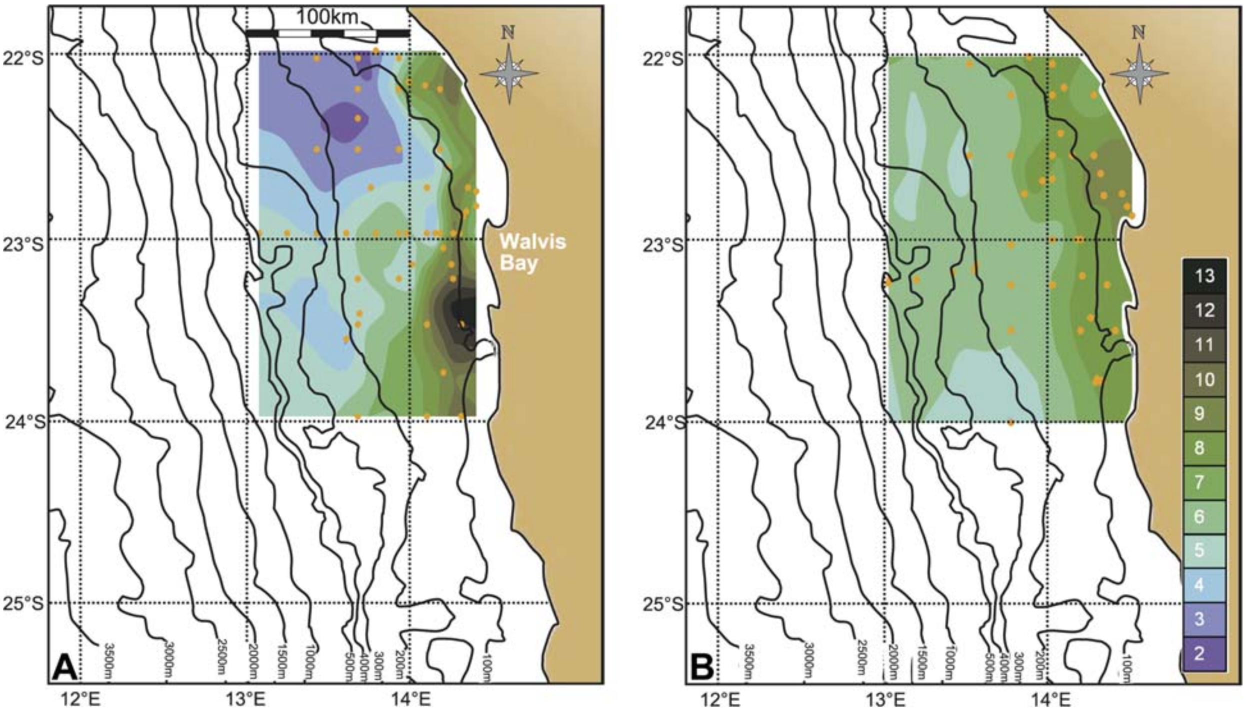

Figure 6. Spatial distribution of surface ocean $\delta^{15}N_{SPM}$ (**A**) and $\delta^{15}N_{sediment}$ (**B**). Note that $\delta^{15}N_{SPM}$ and $\delta^{15}N_{sediment}$ (in ‰) decrease in tandem with increasing distance offshore. The sediment exhibits a smaller isotopic range (4.8 to 11.6 ‰) than SPM (0.8 to 16.1 ‰).

(Libes & Deuser 1988)). Highest values are found in the coastal waters at 23.5° S (Fig. 6A).

With increasing depth, SPM generally exhibits increasing $\delta^{15}N$-signatures. Different mechanisms seem to operate in close proximity to the coast, where $\delta^{15}N_{SPM}$ often declines with depth (Figs 3A, D).

Surface sediments

$\delta^{15}N_{sediment}$. The spatial distribution of $\delta^{15}N_{sediment}$ was extrapolated from nearly one hundred measurements taken between latitude 19 and 30° S as far as 1° E (Figs 7, 8). Highest $\delta^{15}N_{sediment}$-values (± 10 ‰) are situated about one degree latitude further north (22.5° S) than maximum surface ocean $\delta^{15}N_{SPM}$ (Fig. 6). Overall, however, $\delta^{15}N_{sediment}$ imitates the oceanward decline in $\delta^{15}N_{SPM}$, reaching a minimum (± 6 ‰) approximately 160 km off the coast (Fig. 7). Interestingly, this distance coincides perfectly with the lower shelf break, situated at an approximate depth of 400 m (Fig. 1 right chart; Shannon 1985; Bremner & Willis 1993). West of the shelf break, the trend of $\delta^{15}N_{sediment}$ is being reversed. Above the continental slope and toward the mesopelagic ocean $\delta^{15}N_{sediment}$ rises continuously (reaching 12 ‰

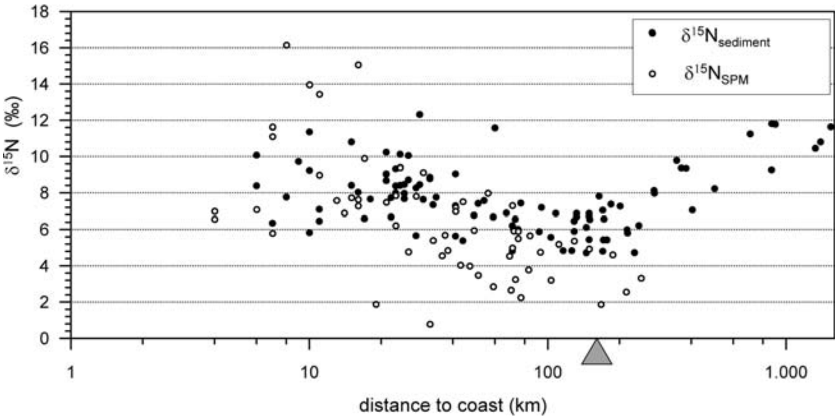

Figure 7. Surface water $\delta^{15}N_{SPM}$ and $\delta^{15}N_{sediment}$ vs. distance to coast. Note the logarithmic scale. The $\delta^{15}N_{SPM}$-records are basically restricted to the shelf between latitude 22 and 25.5° S. Delta$^{15}N_{sediment}$ covers a much broader coastal section (19 to 30° S) and reach far over the continental slope more than 1000 km offshore (for a map view see Figure 8). Note the reversal of trend above the lower shelf break, marked by the triangle, in approximately 160 km distance to the coast.

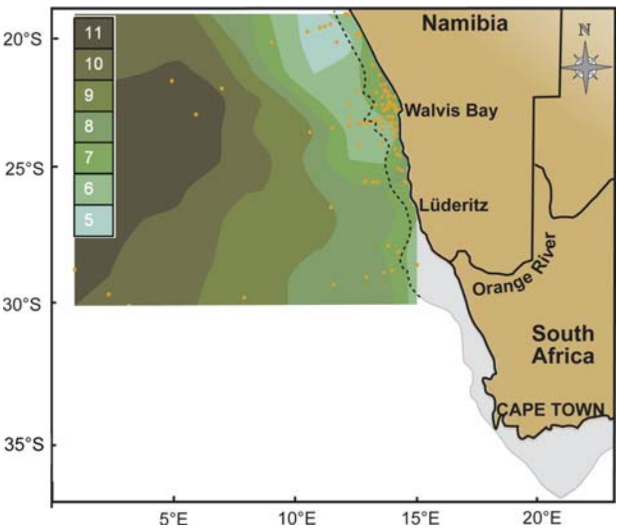

Figure 8. Spatial distribution of $\delta^{15}N_{sediment}$ (in ‰). The larger scale shows that the previously observed oceanward decrease in $\delta^{15}N_{sediment}$ (Fig. 6B) is restricted to the shelf. Beyond the shelf edge (marked by the dotted line), the sediments exhibit continuously rising $\delta^{15}N_{sediment}$-values (see also Fig. 7).

1500 km off the coast). Unfortunately, we lack $\delta^{15}N_{SPM}$-data for comparison (Figs 7, 8) (NB: The $\delta^{15}N_{sediment}$-range is more or less comparable to values from the Peru Upwelling (Libes & Deuser 1988)).

UK'37-temperature. As expected, UK'37-derived SST-records reflect the seasonal upwelling in the vicinity of Walvis Bay (corresponding to the Central Namibian Cell) much better than the CTD-measurements, which were taken during slackened upwelling (Fig. 2). The UK'37-derived SST-range shown in Figure 2 (~ 12.5 to 20 °C) is markedly similar to the SST-range observed through direct measurements (~ 12.5 to 19 °C).

Total organic carbon. [TOC] ranges from less than 0.1 to 19 % by weight (Fig. 4B). Coastal sediments exhibit particularly variable concentrations and above the middle shelf, data are sparse. Contrary to surface water SPM (Fig. 4A), the oceanward decline in organic matter is not clearly obvious in sedimentary [TOC]. It is only beyond the shelf break, i.e. above the upper slope, that [TOC] displays a clear oceanward decline.

Varying amounts of diluents such as carbonate, siliceous matter, etc. may account for the great range of [TOC] above the inner shelf and contribute to the lacking trend (Fig. 4A). The fuzziness of coastal [TOC] nonetheless, UK'37-temperatures and [TOC] perform a rather clear inverse correlation (Fig. 9).

Discussion

Vertical variation of $\delta^{15}N_{SPM}$ and comparing surface ocean $\delta^{15}N_{SPM}$ with $\delta^{15}N_{sediment}$

The comparison of $\delta^{15}N$-signatures in SPM with the underlying sediment shows if, or the extent to which, secondary processes blur the original pelagic signal. The better we understand such processes, the more valuable our interpretation of isotopic variations in ancient sediments.

Unaltered $\delta^{15}N_{SPM}$- and $\delta^{15}N_{sediment}$-signals are anticipated to reflect the isotopic signatures of the first trophic level. Given the excess of phytoplankton biomass, the influence of higher trophic levels (i.e. zooplankton) is considered negligible. This is particularly true for the inner shelf, where the large quantity of primary producers dilutes any other isotopic influence. The same argument applies to the influence of terrestrial material introduced by winds as dust. Due to the absence of a major river draining into the ocean, significant fluvial input can be ruled out a priori (Holmes et al. 1998; Tyrrell & Lucas 2002). Molar C_{org}/N ratios in surface water SPM (spanning 6.6 to 13.6; see Figure 3 although only a selection of surface ocean C_{org}/N ratios are shown there) further support the primarily marine nature of the particles (Redfield 1934; Schubert & Calvert 2001).

Admittedly, the comparison of $\delta^{15}N_{sediment}$ with $\delta^{15}N_{SPM}$ is not ideal. $\delta^{15}N_{sediment}$ represents a time-integrated signal while $\delta^{15}N_{SPM}$ has a rather instantaneous character. Outliers and the strong seasonal imprint account for the larger isotopic range of the latter (Libes

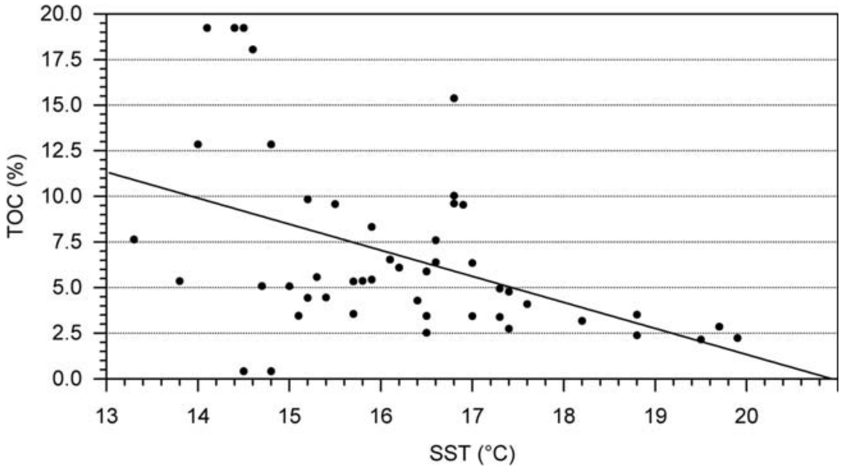

Figure 9. SST (alkenone-based) vs. sedimentary [TOC]. The inverse correlation ($r^2 = 0.21$; $p = 0.141\,\%$) agrees with highest primary production in coastal proximity where the pristine pool of cold and nutrient-rich waters upwells. The majority of data pairs derives from the shelf between latitude 19 and 25.5° S.

& Deuser 1988; Montoya 1994). Long-term sediment trap studies integrate seasonal fluctuations signals and would be more appropriate than filtration-based SPM. As a matter of fact, intense fishing activities inhibit an area-wide deployment of moorings, which is why we have to content ourselves with the filtration-based "snapshot" signal.

Given the extremely dynamic nature of the system including the interaction of longshore and cross-shelf water movements, this "snapshot" character of $\delta^{15}N_{SPM}$ should definitively be kept in mind. Rapid changes are common to the system (e.g. Shannon 1985; Shannon & O'Toole 1998; Brüchert et al. 2004) and samples taken in one year certainly cannot be generalised to the next or even other seasons. In the shallow inner shelf region, short-term variability is particularly pronounced due to strong vertical water movements associated with the coastal upwelling.

Also note that the samples were taken off the main upwelling season, when $\delta^{15}N$ is expected to already have shifted towards higher values as a result of advanced nutrient depletion. Within 20 km off the coast, this 'end-of-bloom' sampling tends to manifests itself in a negative offset between $\delta^{15}N_{sediment}$ and surface ocean $\delta^{15}N_{SPM}$, i.e. $\delta^{15}N_{SPM}$ exceeding $\delta^{15}N_{sediment}$ (Fig. 10). The recent addition of denitrified ^{15}N-enriched nitrate to the surface water masses represents an alternative explanation.

Nearshore stations often exhibit declining $\delta^{15}N_{SPM}$-values with increasing depth (Figs 3A, D). This contradicts the idea of remineralisation in the water column. It is a popular belief that microbial degradation produces elevated $\delta^{15}N$-signatures in the residual OM as a result of discrimination against ^{15}N during metabolic reactions (e.g. Melander 1960; Gaebler et al. 1966; Saino & Hattori 1980; Altabet & McCarthy 1985; Schäfer & Ittekkot 1993; Altabet & Francois 1994; Montoya 1994; Ostrom et al. 1997; Sachs & Repeta 1999). Still, the observation that the $\delta^{15}N$-signature of OM may also decline is not new (e.g. Altabet et al. 1991; Gaye-Haake et al. 2005). Some authors mention the ingrowth of bacteria (containing low $\delta^{15}N$) as a potential candidate capable of efficiently counteracting the effects of remineralisation (Libes & Deuser 1988; Holmes et al. 1999; Lehmann et al. 2002).

Another possible explanation for the depth-related decline in $\delta^{15}N_{SPM}$ is based on the 'end-of-bloom' sampling: Assuming that the particles do not undergo any $\delta^{15}N$-relevant alteration while sinking, the downward gradient would simply mirror the typical course of a phytoplankton bloom, i.e. the progressive ^{15}N-enrichment of surface ocean organic matter, with subsurface $\delta^{15}N_{SPM}$-signals corresponding to older surface signals. In other words, if the transfer of SPM to the ocean floor is too fast for biochemical processes to leave an imprint, low $\delta^{15}N_{SPM}$ in deeper waters reflect surface water conditions at an earlier, i.e. less nutrient-depleted state.

How is it, however, that the material only escapes degradation in coastal vicinity? Both the depth-related decline in $\delta^{15}N$ and the negative offsets between $\delta^{15}N_{sediment}$ and $\delta^{15}N_{SPM}$ are predominantly found within 20 km off the coast. Further offshore, $\delta^{15}N_{SPM}$ rises with depth (Figs 3C, E–F) and sediments are nearly universally ^{15}N-enriched compared to surface ocean suspended matter (Fig. 10). Here, remineralisation, or rather, NH_3-outgassing seems to effectively influence the $\delta^{15}N_{SPM}$-signal.

In the shallow inner shelf waters, a combination of several aspects seems to promote the preservation of the original signal. High primary production and correspondingly high particle concentrations induce the formation of bigger and fast sinking aggregates (Figs 4, 5). Both the short transit to the bottom as well as rapid burial after deposition contributes to the preservation of the original signal (Libes & Deuser 1988; Altabet et al. 1991; Montoya 1994; Ostrom et al. 1997; Altabet et al. 1999; Holmes et al. 2002). The lack of oxygen moreover inhibits diagenetic alteration (e.g. Altabet et al. 1999; Sachs & Repeta 1999). Note that sampling took

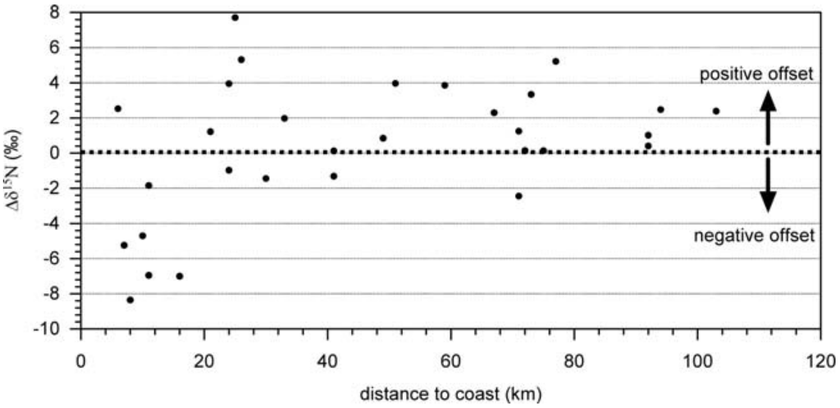

Figure 10. Offset between $\delta^{15}N_{sediment}$ and surface ocean $\delta^{15}N_{SPM}$ ($\Delta\delta^{15}N = \delta^{15}N_{sediment} - \delta^{15}N_{SPM}$) vs. distance to coast. Samples of the data pairs are restricted to the region between latitude 22 and 25.5° S. Above the innermost shelf, the sediments tend to contain lower $\delta^{15}N$-signatures than surface water SPM, hence the negative $\Delta\delta^{15}N$-values. This observation might result from 'end-of bloom' sampling and/or the recent upwelling of denitrified nitrate.

place during austral summer, when the O_2-deficiency above the inner shelf is particularly pronounced due to the higher percentage of hypoxic SACW. In fact, during Meteor cruise M57–3 the inner shelf bottom waters exhibited zero oxygen (Brüchert et al. 2004). Other studies conducted at that time of the year report similar circumstances (e.g. Lavik et al. 2009).

Above the outer shelf, OM is much more liable to degradation for several reasons. Due to greater depths and lower sedimentation rates, the residence time in the water column increases. This fact greatly enhances the particulates' exposure and susceptibility to microbial activity (e.g. Holmes et al. 1999). Besides that, little vertical flux comes along with lower local oxygen consumption. The greater influence of oxygen-rich ESACW towards the west further contributes to the better ventilation above the outer shelf (Brüchert et al. 2004; Lavik et al. 2009). As a matter of fact, the rising susceptibility to diagenesis with increasing distance to the coast (as inferred from the $\delta^{15}N_{SPM}$-profiles) agrees well with the zonal bottom O_2-gradient.

Spatial trends and relationships between proxy indicators

A number of studies conducted in the northern Benguela reported decreasing $[NO_3^-]$ and concomitantly increasing $\delta^{15}N$-signatures with increasing distance to the coast (e.g. Conkright et al. 1998; Holmes et al. 1998, 1999, 2002). These observations are consistent with the idea of nutrient-rich waters coming to the surface along the coast, being dragged offshore by Ekman transport and, according to the concept of Rayleigh fractionation kinetics, becoming more and more depleted in ^{14}N-NO_3^- along the way.

Until now, however, the majority of studies (including the ones mentioned above) has dealt with the continental slope and only minor attention has been paid to the shelf. Here, $\delta^{15}N$-values behave precisely opposite to the expected pattern. Both sediments and suspended particles exhibit a westward decline in $\delta^{15}N$, reaching a minimum above the edge of the shelf (Fig. 7).

The coastal $\delta^{15}N$-maximum has already been mentioned by Pichevin et al. (2005) and Emeis et al. (2009). Comparing two multicores, one from the inner and one from the outer shelf, Struck et al. (2002) found the former exhibiting higher $\delta^{15}N$-values. As a matter of fact, the mechanisms are still far from being understood. In the following we are going to propose a model that might account for the unexpected spatial pattern of $\delta^{15}N$. At the same time, the applicability of $\delta^{15}N_{sediment}$ as a proxy of past nitrogen cycling in the northern Benguela is reassessed.

Denitrification and the $\delta^{15}N$-maximum along the coast

When oxygen consumption exceeds the oxygen concentration of the source water, anaerobic decomposition starts in the form of denitrification (Mohrholz et al. 2008). Denitrifying microbes use nitrate instead of oxygen in order to oxidise OM and are observed to become dominant only when oxygen drops below 0.2 ml/l (Bubnov 1972; Cline & Kaplan 1975; Knowles 1982; Packard et al. 1983).

The oxygen deficiency results from a combination of high remineralisation supported by the initially O_2-rich ESACW on its pathway up the shelf as well as high fractions of O_2-poor SACW. Local oxygen consumption due to high organic particle flux further contributes to the high O_2-demand and O_2-depletion in the bottom waters. In fact, denitrification tends to be associated with high primary production rates (e.g. Tyrrell & Lucas 2002).

Denitrifying bacteria discriminate against ^{15}N. As a consequence, the residual NO_3^--pool becomes progressively enriched in ^{15}N by several per mil. Once this ^{15}N-enriched nitrate is carried to the photic zone, it is assimilated by the plankton, thus initiating a shift towards higher $\delta^{15}N$-signals in the primary products (Cline & Kaplan 1975; Montoya 1994; Holmes et al. 1996). As a consequence, denitrification not only brings about immense nitrogen loss but also strongly interferes with the isotopic record.

In actual fact, coastal $\delta^{15}N_{SPM}$ and $\delta^{15}N_{sediment}$ exhibit values exclusively higher than 5.5 ‰ (Fig. 7), which is the average isotopic signature of the source water nitrate (Sigman et al. 1997, 2000; Ren et al. 2009). Given the proximity to the nutrient source and upwelling, prior consumption can hardly be held responsible for this ^{15}N-enrichment. Second, the central Namibian shelf exhibits pronounced nitrate deficits in coastal proximity (Tyrrell & Lucas 2002; Kuypers et al. 2005). The nitrate deficits (i) in combination with the coastal-parallel belt of high $\delta^{15}N_{SPM}$ and $\delta^{15}N_{sediment}$ (ii) (Figs 6, 7), high flux rates (iii) (Figs 4A, 5), and the oxygen depletion in the bottom waters (iv), unanimously support the influence of denitrification in the source waters (see also Pichevin et al. 2005; Emeis et al. 2009; Lavik et al. 2009). Based on a number of nutrient profiles taken at selected stations during Meteor cruise M57–3, Brüchert et al. (2004) were able to locate the zones of denitrification along the water column.

We shall mention that Kuypers et al. (2005) believe in anammox (anaerobic ammonium oxidation by nitrate and/or nitrite to yield N_2) rather than denitrification as the main process behind the observed nitrogen deficit in the shelf waters. As far as we know, no study has yet examined whether or not annamox is associated with nitrogen isotope fractionation. Without this knowledge, the ultimate reason for the coastal ^{15}N-enrichment remains open to discussion and the influence of a process other than denitrification cannot be ruled out.

Delta^{15}N vs. [TOC] and $\delta^{15}N$ vs. SST

Given the contemporaneous westward decrease in primary production and shelf $\delta^{15}N$-values (Figs 4, 6), we expected [TOC] and $\delta^{15}N_{sediment}$ to be positively corre-

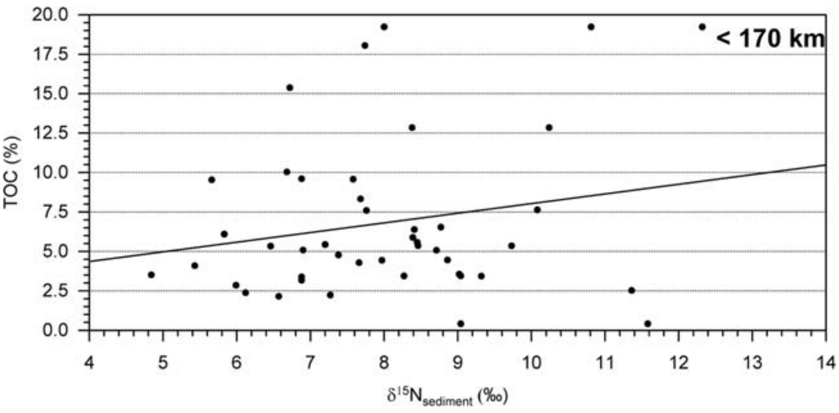

Figure 11. Delta$^{15}N_{sediment}$ vs. [TOC]. Data pairs are restricted to the continental shelf (< 170 km distance to the coast) between latitude 19.0 and 25.5° S. High primary production, as indicated by high [TOC], tends to be associated with high $\delta^{15}N$-values. The observed relation of $\delta^{15}N_{sediment}$ and [TOC] is neither pronounced nor statistically significant ($r^2 = 0.04$; $p = 18.10\,\%$). However, it does not strictly follow Rayleigh fractionation kinetics either but rather suggests the influence of denitrification.

lated within 170 km off the coast. In fact, the great range of coastal [TOC] (Fig. 4B) largely obliterates the anticipated relationship. The remaining correlation is nearly negligible (Fig. 11), but still corroborates the presence of denitrified source waters.

Above the continental slope, the relationship is being reversed and lower $\delta^{15}N$-signals correlate with higher [TOC] (Holmes et al. 1998). The coincidence of minimum $\delta^{15}N$ (Fig. 7) and elevated [TOC] right above the edge of the shelf (Fig. 4B) supports these findings. Holmes et al. (1998) interpreted the negative correlation as the direct response to relative nitrate consumption and Rayleigh fractionation kinetics.

This interpretation, however, is valid on two assumptions only: Firstly, relative nitrate utilisation represents the only significant process acting on the $\delta^{15}N$-signature of nitrate ($\delta^{15}N_{nitrate}$). Secondly, nitrate is not in limited supply as phytoplankton only discriminates between the heavy and light isotopes as long as nutrients are abundant (Ostrom et al. 1997). Both prerequisites turn out problematic where denitrification plays a prominent role (denitrification acts as a nitrate sink and

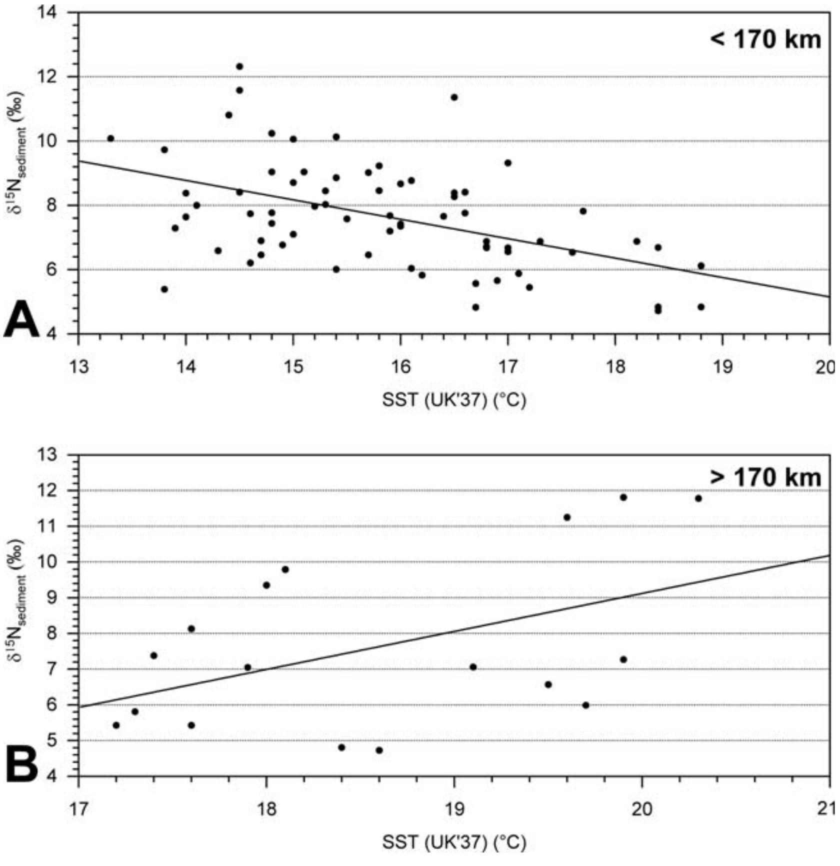

Figure 12. SST (alkenone-based) vs. $\delta^{15}N_{sediment}$ between latitude 19 and 26.5° S. **A.** The negative correlation above the continental shelf (< 170 km off the coast) corresponds to the upwelling of cold and denitrified (i.e. ^{15}N-enriched) source waters ($r^2 = 0.23$; $p = 0.01\,\%$); **B.** Beyond the shelf edge, the trend reverses ($r^2 = 0.22$; $p = 5.2\,\%$).

enriches the remaining pool in ^{15}N at the same time) and thus hardly apply to the inner shelf region, where photic zone [NO_3^-] often approximates near-zero levels (Tyrrell & Lucas 2002; Lavik et al. 2009).

As with [TOC] and $\delta^{15}N_{sediment}$, the relationship between SST and $\delta^{15}N_{sediment}$ reverses west of the shelf break (Fig. 12). In coastal proximity, low SSTs and concomitantly high $\delta^{15}N_{sediment}$-values testify to the upwelling of cold and denitrified source waters (Emeis et al. 2009). The negative correlation between SST and $\delta^{15}N_{sediment}$ only concerns the continental shelf though. Beyond 170 km offshore, both parameters increase in tandem. Even though the latter finding is only supported by a limited data set herein, it agrees well with the results presented by Holmes et al. (1999).

Potential reasons for the $\delta^{15}N$-minimum at the shelf break

Potential reasons for low $\delta^{15}N$-signals in the primary product include (i) nitrogen fixation by cyanobacteria, (ii) diatom-mediated, vertical nutrient transport (Villareal et al. 1993) and (iii), according to the concept of Rayleigh fractionation kinetics, abundant nitrate supply. To our knowledge, no evidence has yet been found that nitrogen fixation plays an important role in the area investigated (see also Emeis et al. 2009). The same applies to vertically migrating diatoms.

The fact that minimum $\delta^{15}N$ coincides that well with the edge of the shelf (Fig. 7) strongly suggests a topographically controlled scenario. Shelf edge upwelling represents a highly promising explanation. Hart & Currie (1960) were the first to advance the idea of two-celled circulation in the northern Benguela region. Since then, various authors have put the hypothesis of shelf edge upwelling further forward (e.g. Bang 1971; Barange & Pillar 1992; Brüchert et al. 2004; Pichevin et al. 2005; Summerhayes et al. 2005; Emeis et al. 2009).

Emeis et al. (2009) reported a narrow band of elevated nitrate concentrations situated above the shelf break between latitude 22 and 24° S. Nutrient replenishment via shelf edge upwelling not only accounts for reduced relative nitrate consumption and a corresponding decline in $\delta^{15}N$ in the primary product, but also fits the increase in primary production, as inferred from the minor peak in [TOC] above the outer shelf and upper continental slope (Fig. 4B). Summerhayes et al. (1995) argue that high concentrations of nutrients and organic particles make shelf edge upwelling a reasonable scenario.

The theory of a two-celled circulation scheme fits our findings reasonably well. The fact that the UK'37-record (Fig. 2B) indicates no shelf break cooling is not automatically considered a counter-argument. Upwelled waters do not necessarily reach the uppermost water layer where the UK'37-record is generated (the UK'37-record derives from phytoplankton dwelling between 0 and 2 m depth; see Emeis et al. 2009). Besides that, shelf edge upwelling does not bring as cold waters to the surface ocean as the coastal upwelling does (Summerhayes et al. 1995).

Potential interplay of oceanographic and nutrient-relevant processes and their control on the local nutrient dynamics

Before going into details we would like to emphasise that the model proposed here is intended to be valid for the area investigated only. So far, we have discussed the coastal $\delta^{15}N$-maximum as well as the shelf break minimum. However, the reason for the actual decline in $\delta^{15}N_{sediment}$ and $\delta^{15}N_{SPM}$ within ± 160 km to the coast is still open. The combination of the following two mechanisms provides a reasonable explanation:

(i) As bottom waters travel up the shelf they get more and more anoxic due to decomposition reactions they are supporting on their way. The proceeding exhaustion of O_2 is accompanied by rising $\delta^{15}N_{nitrate}$-values because denitrification gets increasingly important as oxygen is gradually used up. Interestingly, the oceanward decline in surface water $\delta^{15}N_{SPM}$ (Fig. 6A) represents an exact copy of the trend bottom $\delta^{15}N_{nitrate}$ is expected to perform. Apparently, bottom nitrate somehow supports primary production in the photic zone over large areas of the continental shelf. An obvious explanation is that the penetration of wind- and wave-induced mixing is so deep as to tap the varyingly denitrified, subsurface waters (Fig. 13). The fact remains, however, that the vertical mixing is not so pronounced as to erase the east-west temperature gradient of the surface waters (Fig. 2B). Coldest SSTs concentrate to a narrow band right at the coast and temperatures increase slightly above the middle shelf. The actual process of upwelling only occurs when the cold bottom waters hit the coast.

(ii) The second feature considered capable of outweighing the ^{15}N-enrichment of surface nitrate as the water masses are dragged offshore is related to shelf edge upwelling. Shelf edge upwelling involves the formation of large eddies and swirls, whose interaction with the westward flowing surface currents is believed to create a zone of turbulence and mixing spreading across the middle shelf (Fig. 13). In this zone, situated roughly between 20 and 170 km off the coast, denitrified ^{15}N-enriched water from the coastal upwelling encounters and mixes with nutrient-rich waters introduced at the shelf edge.

The scenario of eddy-induced, cross-shelf mixing corresponds well with the random distribution of [NO_3^-] across the shelf, shown by Tyrrell and Lucas (2002). The fact is, however, that their compilation combines [NO_3^-]-data from a wide range of depths and the question arises whether the trend would still be lacking if only surface [NO_3^-] be considered.

So far, there is no adequate set of [NO_3^-]-data to test our hypotheses against. On the basis of the available facts we incline to the view that the westward de-

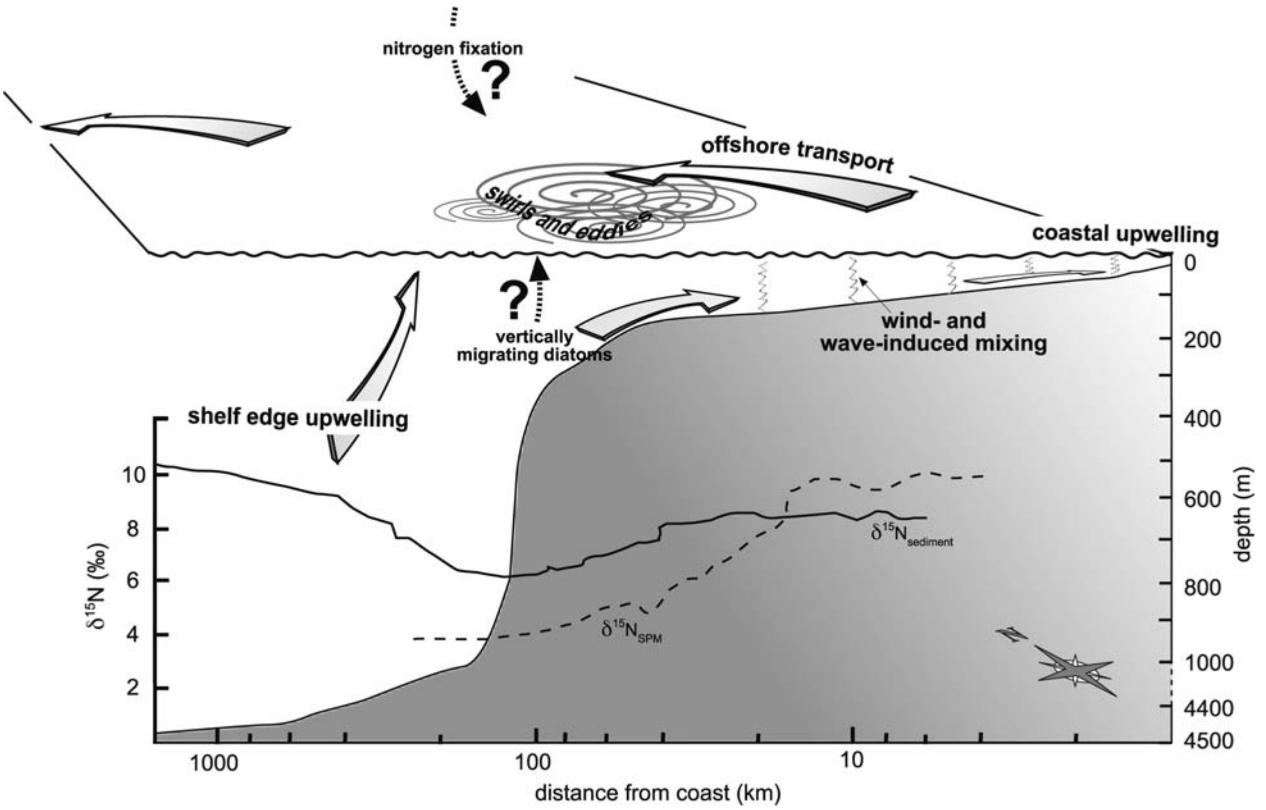

Figure 13. Model showing the potential factors controlling the nutrient dynamics above the shelf. The decline in δ^{15}N toward the outer shelf (see Fig. 7) may partially be ascribed to shelf edge upwelling and the formation of large eddies and swirls creating a zone of mixing spreading across the shelf. In this zone, westward propagating waters from the coastal upwelling (denitrified, i.e. ^{15}N-enriched) encounter and mix with nutrient-rich waters introduced via shelf edge upwelling. Vigorous wind- and wave-induced mixing and the resultant introduction of denitrified bottom waters to the photic zone represents an alternative scenario that might account for the δ^{15}N-gradient. Indirect nutrient supply, mediated by organisms such as vertically migrating diatoms or nitrogen-fixing cyanobacteria, may contribute to the δ^{15}N minimum above the shelf edge.

crease in $\delta^{15}N_{sediment}$ and surface ocean $\delta^{15}N_{SPM}$ results from decreasing relative nitrate consumption, based on a combination of less primary production (the vertical flux declines; Fig. 4) and replenished nutrient supplies. The replenishment with nutrients occurs via shelf edge upwelling (hypothesis ii) as well as the mixing of subsurface nitrate into the surface layer over large areas of the shelf (hypothesis i), with both mechanisms working against the expected nutrient drawdown as surface waters travel offshore.

As outlined above, terrestrial material has no measurable effect. Some might argue nonetheless that, with increasing distance to the coast and concomitantly declining primary production rates (Fig. 4), terrigenous nitrogen (i.e. ammonium bound in clays; Bremner & Willis 1993) could gain proportionally enough importance to lower the bulk δ^{15}N-signal. Dust from southern Africa exhibits comparably low δ^{15}N-values (± 5 ‰; Holmes et al. 2002) and could contribute, therefore, to the observed decline in δ^{15}N. However, C_{org}/N of surface ocean suspended matter argues against this hypothesis. C_{org}/N values are a widely used instrument in distinguishing between marine and terrestrial organic matter (Schubert & Calvert 2001). If terrestrial matter would increase relative to marine material, C_{org}/N should increase. In fact, C_{org}/N ratios are randomly distributed (not shown).

The rise in $\delta^{15}N_{sediment}$ beyond the shelf agrees with earlier studies and is usually ascribed to the steady ^{15}N-enrichment of the nitrate pool as it is drawn down by phytoplankton growth (Holmes et al. 1996, 1998, 1999; Pichevin et al. 2005). Still, the translation of $\delta^{15}N_{sediment}$-values into nitrate consumption remains debatable. As microbial impact increases along with depth, the oceanward rise in $\delta^{15}N_{sediment}$ may also be ascribed to the increasing influence of organic matter decay, or rather, NH_3-outgassing (Meisel & Struck 2011).

As long as we lack surface ocean $\delta^{15}N_{SPM}$-data from the continental slope, the topic remains open to discussion. In case that surface water $\delta^{15}N_{SPM}$ copies the rise performed by $\delta^{15}N_{sediment}$, the development of $\delta^{15}N_{sediment}$ might primarily be Rayleigh-controlled. An increasing offset between surface water and sedimentary δ^{15}N would rather account for degradation-controlled $\delta^{15}N_{sediment}$, instead. Analysing δ^{15}N on rinsed sediment represents an alternative in order to detect the influence of microbial impact (Meisel & Struck 2011). Rinsing prior to measurement seems capable of restoring the original pelagic signal, wiping out decayal-related δ^{15}N-shifts (Meisel & Struck 2011).

Conclusions and outlook

Surface ocean $\delta^{15}N_{SPM}$-data substantiate the previously observed $\delta^{15}N_{sediment}$-gradient above the central Namibian shelf (i.e. decreasing $\delta^{15}N$-signals towards the shelf edge). On the evidence of the strikingly parallel trend of $\delta^{15}N_{sediment}$ and $\delta^{15}N_{SPM}$, secondary processes such as microbial activity are apparently not so pronounced as to obliterate the surface-generated signal. The downward transfer of unaltered surface production seems to work particularly well in the shallow coastal waters where the flux is high and fast. However, in order that $\delta^{15}N_{sediment}$ can be a reliable tool in the study of palaeo-oceanography, it is not only the link between the surface production and the sedimentary record that needs to be demonstrated. In fact, the parameter only becomes useful if the processes producing the surface signal are known. Main uncertainties stem from the potential influence of denitrified waters as well as the apparent, yet unsubstantiated, introduction of nutrient-rich water at the shelf edge and its mixing into the original pool along its flow path. The deep penetration of wind- and wave-induced mixing and the tapping of varyingly denitrified bottom waters appear to be additional characteristics of the shallow shelf. All these factors complicate the local nitrogen budget and should be kept in mind when interpreting $\delta^{15}N$-fluctuations in sediment cores retrieved from this area.

The apparent lack of any relationship between $\delta^{15}N$ and $[NO_3^-]$ casts doubt on the applicability of $\delta^{15}N$ as a reliable proxy of relative nutrient utilisation above the central Namibian shelf. Much effort is currently being put in the data mining of large amounts of surface $[NO_3^-]$-measurements and shelf-wide $[NO_3^-]$-profiles, including isotopic analysis ($\delta^{15}N_{nitrate}$). This will help to identify the sources contributing to today's nutrient regime and will highly improve the interpretation of the $\delta^{15}N_{sediment}$-pattern as well as advance our understanding of the single processes involved (i.e. shelf edge upwelling, nitrogen fixation, etc.).

Acknowledgements

The authors thank Ewgenija Kuhl, Nina Holzner and Michelle Mohr for sample preparation and taking measurements. We are furthermore indebted to Cameron Paul for proof-reading. Finally, we would also like to thank the reviewers for their useful comments and suggestions that helped to improve the manuscript. The research was funded by the German Research Foundation (DFG) in the frame of the project STR356/3.

References

Altabet, M. A. & McCarthy, J. J. 1985. Temporal and spatial variations in the natural abundance of ^{15}N in PON from a warm-core ring. – Deep-Sea Research 32: 755–772.

Altabet, M., Deuser, W. G., Honjo, S. & Stienen C. 1991. Seasonal and depth-related changes in the source of sinking particles in the North Atlantic. – Nature 354: 136–139.

Altabet, M. A. & Francois, R. 1994. Sedimentary nitrogen isotopic ratio as a recorder for surface ocean nitrate utilization. – Global Biogeochemical Cycles 8: 103–116.

Altabet, M. A., Pilskaln, C., Thunnel, R., Pride, C., Sigman, D., Chavez, F. & Francois, R. 1999. The nitrogen isotope biogeochemistry of sinking particles from the margin of the Eastern North Pacific. – Deep Sea Research I 46: 655–679.

Bakun, A. & Weeks, S. J. 2004. Greenhouse gas buildup, sardines, submarine eruptions and the possibility of abrupt degradation of intense marine upwelling ecosystems. – Ecology Letters 7: 1015–1023.

Bang, N. D. 1971. The southern Benguela current region in February, 1966: Part II. Bathythermography and air-sea interactions. – Deep-Sea Research 18: 209–224.

Barange, M. & Pillar, S. C. 1992. Cross-shelf circulation, zonation and maintenance mechanisms of *Nyctiphanes capensis* and *Euphausia hanseni* (Euphausiacea) in the northern Benguela upwelling system. – Continental Shelf Research 12 (9): 1027–1042.

Berger, W. H., Smetacek, V. S. & Wefer, G. 1989. Productivity of the ocean: present and past. John Wiley & Sons, Chichester.

Berger, W. H. & Wefer, G. 2002. On the reconstruction of upwelling history: Namibia upwelling in context. – Marine Geology 180: 3–28.

Boebel, O., Lutjeharms, J., Schmid, C., Zenk, W., Rossby, T. & Barron, C. 2003. The Cape Cauldron: a regime of turbulent inter-ocean exchange. – Deep-Sea Research 2 (50): 57–86.

Bremner, J. M. & Willis, J. P. 1993. Mineralogy and geochemistry of the clay fraction of sediments from the Namibian continental margin and the adjacent hinterland. – Marine Geology 115: 85–116.

Brüchert, V., Altenbach, A. V., Bening, G., Bockelmann, F., Currie, B., Donath, J., Dübecke, J., Endler, R., Erdmann, S., Ertan, T., Fuchs, B., Klockgether, G., Krüger, S., Kuypers, M. M. M., Lass, H. U., Lavik, G., Lilienthal, S., Leipe, T., Nickel, G., Noli-Peard, K., Ohde, T., Schulz, B., Schulz, H., Siegel, H., Struck, U., Wulf, J., Zitzmann, S. & Zonneveld, K. 2004. The Benguela Upwelling System 2003, Part 3, Cruise No. 57, Leg 3, March 15 – April 13, 2003, Walvis Bay, Namibia – Dakar. – Meteor Berichte 4: 1–53.

Bubnov, V. A. 1972. Structure and characteristics of the oxygen minimum layer in the southeast Atlantic Ocean. – Oceanology 12: 193–201.

Calvert, S. E. & Price, N. B. 1971. Upwelling and nutrient regeneration in the Benguela Current, October, 1968. – Deep-Sea Research 18: 505–523.

Chapman, P. & Shannon, L. 1985. The Benguela ecosystem Part II. Chemistry and related processes. – Oceanography and Marine Biology Annual Review 23: 183–251.

Chapman, P. & Shannon, L. 1987. Seasonality in the oxygen minimum layers at the extremities of the Benguela system. – South African Journal of Marine Science 5: 51–62.

Cline, J. D. & Kaplan, I. R. 1975. Isotopic fractionation of dissolved nitrate during denitrification in the eastern tropical North Pacific Ocean. – Marine Chemistry 3: 271–299.

Codispoti, L. & Christensen, J. P. 1985. Nitrification, denitrification and nitrous oxide cycling in the eastern tropical South Pacific Ocean. – Marine Chemistry 16: 277–300.

Conkright, M., O'Brien, T., Levitus, S., Boyer, T. P., Antonov, J. & Stephens, C. 1998. World Ocean Atlas 1998. Vol. 10: Nutrients and Chlorophyll of the Atlantic Ocean. NOAA Atlas NESDIS 36.U.S. Gov. Printing Office, Washington D.C.

Emeis, K.-C., Brüchert, V., Currie, B., Endler, R., Ferdelman, T., Kiessling, A., Leipe, T., Noli-Peard, K., Struck, U. & Vogt, T. 2004. Shallow gas in shelf sediments of the Namibian coastal upwelling ecosystem. – Continental Shelf Research 24 (6): 627–642.

Emeis, K.-C., Struck, U., Leipe, T. & Ferdelman, T. G. 2009. Variability in upwelling intensity and nutrient regime in the coastal upwelling system offshore Namibia: results from sediment archives. – International Journal of Earth Sciences 98: 309–326.

Francois, R., Altabet, M. A. & Burckle, L. H. 1992. Glacial to interglacial changes in surface nitrate utilization in the Indian sector of the southern ocean as recorded by sediment δ^{15}N. – Paleoceanography 7: 589–606.

Gaebler, O. H., Vitti, T. G. & Vukmirovich, R. 1966. Isotope effects in metabolism of ^{14}N and ^{15}N from unlabeled dietary proteins. – Canadian Journal of Biochemistry 44: 1249–1257.

Gaye-Haake, B., Lahajnar, N., Emeis, K.-C., Unger, D., Rixen, T., Suthhof, A., Ramaswamy, V., Schulz, H., Paropkari, A. L., Guptha, M. V. S. & Ittekkot, V. 2005. Stable nitrogen isotopic ratios of sinking particles and sediments from the northern Indian Ocean. – Marine Chemistry 96: 243–255.

Gordon, A. L. 1986. Interocean Exchange of Thermocline Water. – Journal of Geophysical Research 91 (C4): 5037–5046.

Hart, T. J. & Currie, R. I. 1960. The Benguela Current. – Discovery Report 31: 123–127.

Holmes, M. E., Müller, P. J., Schneider, R. R., Segl, M., Pätzold, J. & Wefer, G. 1996. Stable nitrogen isotopes in Angola Basin surface sediments. – Marine Geology 134: 1–12.

Holmes, M. E., Müller, P. J., Schneider, R. R., Segl, M. & Wefer, G. 1998. Spatial variations in euphotic zone nitrate utilization based on δ^{15}N in surface sediments. – Geo-Marine Letters 18 (1): 58–65.

Holmes, B., Eichner, C., Struck, U. & Wefer, G. 1999. Reconstructions of surface ocean nitrate utilization using stable nitrogen isotopes in sinking particles and sediments. *In* Fischer, G. & Wefer G. (eds). Use of Proxies in Paleoceanography: Examples from the South Atlantic. Springer, Berlin: pp. 447–468.

Holmes, E., Lavik, G., Fischer, G., Segl, M., Ruhland, G. & Wefer, G. 2002. Seasonal variability of δ^{15}N in sinking particles in the Benguela upwelling region. – Deep-Sea Research I 49: 377–394.

Knowles, R. 1982. Denitrification. – Microbiological Reviews 46 (1): 43–70.

Kuypers, M. M. M., Lavik, G., Woebken, D., Schmid, M., Fuchs, B. M., Amann, R., Jørgensen, B. B. & Jetten, M. S. M. 2005. Massive nitrogen loss from the Benguela upwelling system through anaerobic ammonium oxidation. – PNAS 102 (18): 6478–6483.

Lavik, G., Krüger, S. & Leipe, T. 2004. CTD Profiling of Nutrients in the Water Column. – Meteor Berichte 4: 20–20.

Lavik, G., Stührmann, T., Brüchert, V., van der Plas, A., Mohrholz, V., Lam, P., Mußmann, M., Fuchs, B. M., Amann, R., Lass U. & Kuypers, M. M. M. 2009. Detoxification of sulphidic African shelf waters by blooming chemolithotrophs. – Nature 459: 581–585.

Lehmann, M. F., Bernasconi, S. M., Barbieri, A. & McKenzie, J. A. 2002. Preservation of organic matter and alteration of its carbon and nitrogen isotope composition during simulated and in situ early sedimentary diagenesis. – Geochimica et Cosmochimica Acta 66: 3573–3584.

Libes, S. M. & Deuser, W. G. 1988. The isotope geochemistry of particulate nitrogen in the Peru Upwelling Area and the Gulf of Maine. – Deep-Sea Research 35 (4): 517–533.

Lutjeharms, J. R. E. & Meeuwis, J. M. 1987. The extent and variability of southeast Atlantic upwelling. – South African Journal of Marine Science 5: 85–94.

Mariotti, A. 1983. Atmospheric nitrogen as a reliable standard for natural 15N abundance measurements. – Nature 303: 685–687.

Meisel, S. & Struck, U. 2011. The potential distortion of sedimentary δ^{15}N and C_{org}/N ratios by NH_4^+ and the effects of pre-analysis sample treatment. – Fossil Record 14 (2): 141–152.

Meisel, S., Emeis, K.-C., Struck, U. & Kristen, I. 2011. Nutrient regime and upwelling in the northern Benguela since the middle Holocene in a global context – a multi-proxy approach. – Fossil Record 14 (2): 171–193.

Melander, L. 1960. Isotope effects on reaction rates. Ronald Press, New York.

Mohrholz, V., Bartholomae, C. H., van der Plas, A. K. & Lass, H. U. 2008. The seasonal variability of the northern Benguela undercurrent and its relation to the oxygen budget on the shelf. – Continental Shelf Research 28 (3): 424–441.

Mollenhauer, G., Schneider, R. R., Müller, P. J., Spieß, V. & Wefer, G. 2002. Glacial/interglacial variability in the Benguela upwelling system: Spatial distribution and budgets of organic carbon accumulation. – Global Biogeochemical Cycles 16 (4): 1134.

Montoya, J. P. 1994. Nitrogen isotope fractionation in the modern ocean: Implications for the sedimentary record. *In* Zahn, R., Pedersen, T. F., Kaminski, M. A. & Labeyrie L. (eds). Carbon Cycling in the Glacial Ocean: Constraints on the Ocean's Role in Global Change, 17, NATO ASI Series. Springer-Verlag, Berlin: pp. 259–279.

Montoya, J. P. & McCarthy, J. J. 1995. Isotopic fractionation during nitrate uptake by phytoplankton growth in continuous culture. – Journal of Plankton Research 17: 439–464.

Moroshkin, K. V., Bubnov, V. A. & Bulatov, R. P. 1970. Water circulation in the eastern South Atlantic Ocean. – Oceanology 10 (1): 27–34.

Nelson, G. & Hutchings, L. 1983. The Benguela upwelling area. – Progress in Oceanography 12: 333–356.

Ostrom, N. E., Macko, S. A., Deibel, D. & Thompson, R. J. 1997. Seasonal variation in the sTable carbon and nitrogen isotope biogeochemistry of coastal cold ocean environment. – Geochimica et Cosmochimica Acta 61 (14): 2929–2942.

Packard, T. T., Garfield, P. C. & Codispoti, L. A. 1983. Oxygen consumption and denitrification below the Peruvian upwelling. *In* Suess, E & Thiede J. (eds). Coastal Upwelling: Its Sediment Record. Plenum Press, New York: pp. 147–173.

Pichevin, L., Martinez, P., Bertrand, P., Schneider, R., Giraudeau, J. & Emeis, K.-C. 2005. Nitrogen cycling on the Namibian shelf and slope over the last two climatic cycles: Local and global forcings. – Paleoceanography 20: 14–24

Poole, R. & Tomczak, M. 1999. Optimum multiparameter analysis of the water mass structure in the Atlantic Ocean thermocline. – Deep-Sea Research I 46: 1895–1921.

Ravelo, A. C. & Fairbanks, R. G. 1992. Oxygen Isotopic Composition of Multiple Species of Planktonic Foraminifera: Recorders of the Modern Photic Zone Temperature Gradient. – Paleoceanography 7 (6): 815–831.

Redfield, A. C. 1934. On the proportions of organic derivatives in sea water and their relation to the composition of plankton. *In* Daniel, R. J. (ed.). James Johnston Memorial Volume, University Press of Liverpool, UK: pp. 176–192.

Ren, H., Sigman, D. M., Meckler, A. N., Plessen, B., Robinson, R. S., Rosenthal, Y. & Haug, G. H. 2009. Foraminiferal Isotope Evidence of Reduced Nitrogen Fixation in the Ice Age Atlantic Ocean. – Science 323: 244–248.

Sachs, J. P. & Repeta, D. J. 1999. Oligotrophy and nitrogen fixation during eastern Mediterranean sapropel events. – Science 286: 2485–2488.

Saino, T. & Hattori, A. 1980. ^{15}N natural abundance in oceanic suspended particulate matter. – Nature 283: 752–754.

Schäfer, P. & Ittekkot, V. 1993. Seasonal variability of δ^{15}N in settling particles in the Arabian Sea and its paleogeochemical significance. – Naturwissenschaften 80: 511–513.

Schubert, C. J. & Calvert, S. E. 2001. Nitrogen and carbon isotopic composition of marine and terrestrial organic matter in Arctic Ocean sediments: implications for nutrient utilization and organic matter composition. – Deep-Sea Research I 48: 789–810.

Shannon, L. V. 1985. The Benguela ecosystem. Part I. Evolution of the Benguela, physical features and processes. – Oceanography and Marine Biology Annual Review 23: 105–182.

Shannon, L. V., Boyd, A. J., Brundrit, G. B. & Taunton-Clark, J. 1986. On the existence of an El Niño-type phenomenon in the Benguela system. – Journal of Marine Research 44 (3): 495–520.

Shannon, L. V. & Nelson, G. 1996. The Benguela: Large Scale Features and Processes and System Variability. *In* Wefer, G., Berger,

W. H, Siedler, D & Webb, D. (eds). The South Atlantic: Present and Past Circulation. Springer, Berlin, Heidelberg: pp. 163–210.

Shannon, L. V. & O'Toole, M. J. 1998. Integrated Overview of the Oceanography and Environmental Variability of the Benguela Current Region: Thematic Report No.2, Synthesis and Assessment of Information on BCLME. October 1998. UNDP, Windhoek.

Shannon, L. V. & O'Toole, M. J., 2003. Sustainability of the Benguela: ex Africa semper aliquid novi. *In* Hempel, G. & Sherman, K. (eds). Large marine ecosystems of the world: trends in exploitation, protection and research. Elsevier B.V., Amsterdam: pp. 227–253.

Sigman, D. M., Altabet, M. A., Michener, R., McCorkle, D. C., Fry, B. & Holmes, R. M. 1997. Natural abundance-level measurement of the nitrogen isotopic composition of oceanic nitrate: an adaption of the ammonia diffusion method. – Marine Chemistry 57 (3–4): 227–242.

Sigman, D. M., Altabet, M. A., McCorkle, D. C., Francois, R. & Fischer, G. 2000. The δ^{15}N of nitrate in the Southern Ocean: nitrogen cycling and circulation in the ocean interior. – Journal of Geophysical Research 105 (C8): 599–614.

Stander, G. H. 1964. The Benguela Current off South West Africa. – Investigational Report of the Marine Research Laboratory of South West Africa 12: 1–43.

Stramma, L. & Peterson, R. G. 1989. Geostrophic Transport in the Benguela Current region. – Journal of Physical Oceanography 19: 1440–1448.

Struck, U., Emeis, K.-C., Alheit, J., Schneider, R., Eichner, C. & Altenbach, A.-V. 2002. Changes of the upwelling rates of nitrate preserved in the δ^{15}N-signature of sediments and fish scales from the diatomaceous mud belt off Namibia. – GeoBios 35: 3–11.

Summerhayes, C. P., Kroon, D., Rosell-Mele, A., Jordan, R. W., Schrader, H.-J., Hearn, R., Villanueva, J., Grimalt, J. O. & Eglington, G. 1995. Variability in the Benguela Current upwelling system over the past 70,000 years. – Progress in Oceanography 35: 207–251.

Tomczak, M. & Godfrey, J. S. 2003. Regional Oceanography: An Introduction. Daya Publishing House.

Tyrrell, T. & Lucas, M. I. 2002. Geochemical evidence of denitrification in the Benguela upwelling system. – Continental Shelf Research 22: 2497–2511.

Villareal, T. A., Altabet, M. A. & Culver-Rymsza, K. 1993. Nitrogen transport by vertically migrating diatom mats in the North Pacific Ocean. – Nature 363: 709–712.

Voss, M., Altabet, M. & von Bodungen, B. 1996. δ^{15}N in sedimenting particles as indicator for euphotic zone processes. – Deep-Sea Research 43: 33–47.

Wada, E. & Hattori, A. 1978. Nitrogen isotope effects in the assimilation of inorganic nitrogenous compounds by marine diatoms. – Geomicrobiology Journal 1: 85–101.

Wada, E. 1980. Nitrogen isotope fractionation and its significance in biogeochemical processes occurring in marine environments. *In* Goldberg, E. D., Horibe, Y. & Saruhashi H. (eds). Isotope Marine Chemistry. Uchida Rokakuho, Tokyo: pp. 375–398.

Waser, N. A. D., Turpin, D. H., Harrison, P. J., Nielsen, B. & Calvert, S. E. 1998. Nitrogen isotope fractionation during uptake and assimilation of nitrate, nitrite, ammonium and urea by a marine diatom. – Limnology and Oceanography 43: 215–224.

Weeks, S. J., Currie, B., Bakun, A. & Peard, K. R. 2004. Hydrogen sulphide eruptions in the Atlantic Ocean off southern Africa: implications of a new view based on SeaWiFS satellite imagery. – Deep-Sea Research I 51: 153–172.